Int. J. Electrochem. Sci., 2 (**2007**) 996 - 1017

International Journal of ELECTROCHEMICAL SCIENCE
www.electrochemsci.org

Temperature Effects on the Corrosion Inhibition of Mild Steel in Acidic Solutions by Aqueous Extract of Fenugreek Leaves

Ehteram A. Noor

King Abd El-Aziz university, Girls College of Education, Chemistry Department, Jeddah, KSA
*E-mail: m7o7o7n@hotmail.com

Received: 21 August 2007 / *Accepted:* 19 September 2007 / *Online published:* 20 October 2007

Gravimetric method was used to study the temperature effects on mild steel corrosion in 2.0M of HCl and H_2SO_4 in the absence and presence of aqueous extract for fenugreek leaves (AEFL). In 2.0 M HCl, the results revealed that the inhibition efficiency of AEFL increases with increasing concentration, but an increase or decrease in the inhibitor efficiency depending on its concentration is detected with increasing temperature. On the other hand, in 2.0 M H_2SO_4, the inhibition efficiency of AEFL was found to increase with increasing both the inhibitor concentration and solution temperature. However, the AEFL inhibited mild steel corrosion in HCl more than in H_2SO_4 at all inhibitor concentrations and solution temperatures. The inhibition action of AEFL was performed via adsorption of the extract species on mild steel surface. The adsorption was spontaneous and followed Langmuir adsorption isotherm in HCl, while followed Temkin adsorption isotherm in H_2SO_4 at all studied temperatures. Thermodynamic data for both inhibitor adsorption and mild steel corrosion led to suggest the occurrence of (a) comprehensive adsorption (physical and chemical adsorption) for the inhibitor species on mild steel from HCl solution and (b) chemical adsorption for the inhibitor species on mild steel from H_2SO_4 solution. The inhibition mechanism for the adsorption of AEFL species on mild steel surface from both acids was discussed with the light of some AEFL constituents.

Keywords: Corrosion; inhibition; mild steel; Fenugreek; gravimetric; Temperature

1. INTRODUCTION

The effect of temperature on a chemical reaction of practical and theoretical important. Like most chemical reactions, the rate of corrosion of iron and steel increases with temperature especially in media in which evolution of hydrogen a companies corrosion, e.g. during corrosion of steel in acids. Acid pickling of steel is usually carried out at elevated temperature─ up to 60°C in hydrochloric acid (HCl) solutions and─ up to 90°C in sulfuric acid (H_2SO_4) solutions [1]. Accordingly, pickling inhibitors are expected to be chemically stable to provide high protective efficiency under the

conditions mentioned above. Temperature effects on acidic corrosion and corrosion inhibition of iron and steel most often in HCl and H_2SO_4 solutions had been the object of a large number of investigations [2-10]. Temperature dependence of the inhibitor efficiency (IE) and the comparison of the obtained thermodynamic data of the corrosion process both in absence and presence of inhibitors leads to some conclusions concerning the mechanism of inhibiting action.

The object of the present work was to study the temperature effects on mild steel corrosion in 2.0 M HCl and 2.0 M H_2SO_4 solutions in the absence and presence of various additions of aqueous extract for fenugreek leaves (AEFL) by using gravimetric method. Various thermodynamic parameters for inhibitor adsorption on mild steel surface were estimated and discussed. Kinetic parameters for mild steel corrosion in absence and presence of the studied inhibitors were evaluated and interpreted. On the light of inhibitor constituent, the inhibition mechanism for mild steel in both acids was suggested.

2. EXPERIMENTAL PART

2.1. Materials

The experiments were performed with mild steel rods of the following composition; C: 0.250, Mn: 0.480, Si: 0.300, Ni: 0.040, Cr: 0.060, Mo: 0.020, S: 0.021, P: 0.019 and the remainder is Fe.

2.2. Preparation of AEFL

Stock solution of the inhibitor extract were prepared by boiling 10 g of dried, grounded fenugreek leaves in 250 ml of de-ionized water for 1 h. The extract was left all night and then filtered and completed to 250 ml by de-ionized water. Both the freshly prepared extract and that aged in a refrigerator for tow months give almost the same results.

2.3. Solutions

The aggressive solutions used were made of AR─ grade (BDH) HCl and H_2SO_4. Appropriate concentration (2.0 M) of each acid was prepared using de-ionized water in the absence and presence of various concentrations of AEFL. The employed concentration range of AEFL was of 0.5-10 v/v % (ml/100ml)

2.4. Corrosion rates measurements

Gravimetric methods was employed for corrosion rates calculations. Prior to each experiment, the mild steel specimen of 1.0 cm in diameter and 5.0 cm in length was abraded with a series of emery paper from 220 to 1000 grades. Then, the specimen was washed several times with de-ionized then with ethanol and dried using a stream of air. After weighing accurately, it was immersed in 100 ml flask, which contained 50 ml of 2.0 M HCl or 2.0 M H_2SO_4 in absence and presence of a certain

concentration of AEFL. After 120 minute, the specimen was taken out, washed, dried and weighed accurately. Then the tests were repeated at different inhibitor concentrations and different temperatures.

3. RESULTS AND DISCUSSION

3.1. Effect of temperature on mild steel corrosion rates

The value of corrosion rate ($\rho_{corr.}$) was calculated from the following equation:

$$\rho_{corr.}(g.cm^{-2}.\min^{-1}) = \frac{m_1 - m_2}{A.t} \quad (1)$$

where m_1 and m_2 are the masses of the specimen before and after corrosion, A is the total area of the specimen and t is the corrosion time.

Table 1 represents the corrosion rates of mild steel specimen in 2.0 M of HCl and H_2SO_4 in the absence and presence of different concentrations of AEFL at different temperatures. As observed from Table 1, the corrosive attack of the uninhibited acids on mild steel surface at all studied temperatures was in the order HCl > H_2SO_4, because of the more corrosive nature of chloride ions. Similar observations were found in previous studies [11-13]. In 2.0 M inhibited HCl solutions, a remarkable decrease in mild steel corrosion rate was observed with the addition of increasing amount of AEFL at each studied temperature. While in 2.0 H_2SO_4 solutions, the low concentration additions (0.5 and 1.0 v/v%) of AEFL causes an acceleration effect especially at temperatures of 30° and 40° C, this behavior disappears with increasing both inhibitor concentration and solution temperature. It is clear from Table 1 that corrosion rate of mild steel in both acids in absence and presence of AEFL obeys the Arrhenius type reactions as it increases with rising solution temperature.

Table 1. Mild steel corrosion rates in 2.0 M of both HCl and H_2SO_4 in absence and presence of different concentrations of AEFL at different temperatures

$C_{inh.}$ (v/v %)	$\rho_{corr} \times 10^5$ (g cm^{-2} min^{-1})									
	HCl					H_2SO_4				
	30°	40°	50°	60°	70°	30°	40°	50°	60°	70°
0.0	1.914	3.142	11.560	19.744	56.832	0.998	2.175	6.896	11.603	36.853
0.5	0.713	1.022	2.986	6.413	29.994	1.163	2.203	5.275	8.865	18.427
1.0	0.382	0.647	2.278	5.480	22.967	1.067	1.715	4.369	5.409	13.281
2.0	0.308	0.563	1.947	3.696	17.546	0.807	1.521	3.914	4.894	9.548
5.0	0.237	0.361	1.105	2.695	7.984	0.741	1.341	3.271	4.115	7.687
10.0	0.180	0.349	1.011	1.735	4.393	0.467	0.817	1.887	3.059	4.301

Assuming that the corrosion rate of mild steel against the concentration of the studied inhibitor obeys the kinetic relationship [14, 15]:

$$\log \rho_{corr.} = \log k + B \log C_{inh.} \quad (2)$$

Where k is the rate constant and equal to $\rho_{corr.}$ at inhibitor concentration of unity, B is the reaction constant which in the present case is a measure for the inhibitor effectiveness and $C_{inh.}$ is the v/v% (ml/100ml) concentration of the AEFL. Figure 1 represents the curves of $\log \rho_{corr.}$ versus $\log C_{inh.}$ at various studied temperatures. The straight lines show that the kinetic parameters (k and B) could be calculated by Eq. 2, and listed in Table 2. The obatained results from this table were summarized as follows:

- The negative sign for the values of reaction constant B indicates that the rate of corrosion process is inversely proportional to the inhibitor concentration, meaning that the inhibitor becomes more effective with increasing its concentration. So, when the change of $\rho_{corr.}$ with inhibitor concentration becomes steep (high negative value for constant B) it reflects good inhibitive properties for the studied inhibitor. Accordingly, by using the value of the constant B, it is possible to compare the inhibitor action in both acids and at different temperatures:
- At all studied temperatures the B values recorded for mild steel in HCl are more negative than these recorded in H_2SO_4, reflecting that AEFL is more effective in the former acid than in the latter.
- Increasing temperature leads to an increase in the inhibitory action of AEFL in both acids except that in HCl solutions as it is observed limited decrease in the negative value of B with increasing temperature from 30° to 50° and after which it tends to become more negative.
- The k value increases with rising temperature in both acids and its magnitude at each temperature for each acid is comparable to that recorded in Table 1 for the analogous system containing 1.0% of AEFL which indicates the validity of Eq. (2).

Table 2. Kinetic parameters for the corrosion of mild steel in 2.0 M of both HCl and H_2SO_4 containing AEFL at different temperatures.

Temperature	Kinetic parameters			
	HCl		H_2SO_4	
(°C)	B	$k \times 10^5$ (g cm^{-2} min^{-1})	B	$k \times 10^5$ (g cm^{-2} min^{-1})
30°	-0.421	0.447	-0.287	1.023
40°	-0.360	0.724	-0.292	1.820
50°	-0.383	2.291	-0.308	4.467
60°	-0.437	5.129	-0.309	5.754
70°	-0.649	22.387	-0.452	13.490

3.2. Effect of temperature on inhibition efficiency IE (%)

With the calculated corrosion rates listed in Table 1, the inhibition efficiency or acceleration for mild steel corrosion in both acids in the presence of various concentrations of AEFL and at different temperatures was obtained from the following equation:

$$IE\ (\%)\ =\ (\frac{\rho^{o}_{corr.}-\rho_{corr.}}{\rho^{o}_{corr.}})\times 100 \qquad (3)$$

where $\rho^{o}_{corr.}$ and $\rho_{corr.}$ are the corrosion rates of mild steel in absence and presence of certain concentration of AEFL, respectively.

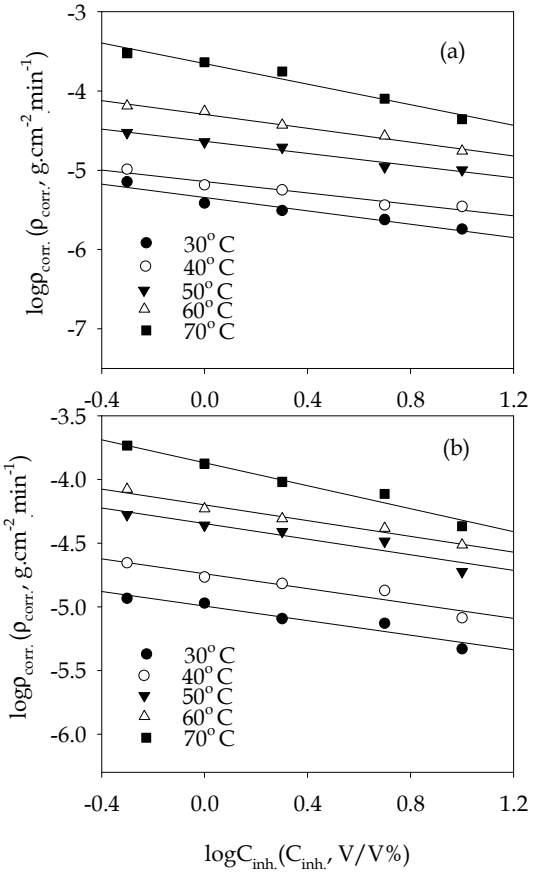

Figure 1. Variation of $\log \rho_{corr.}$ with $\log C_{inh.}$ for mild steel corrosion in (a) 2.0 M HCl and (b) 2.0 H_2SO_4 at various temperatures.

Table 3. Inhibition efficiencies of AEFL at different concentrations and temperatures in 2.0 M of both HCl and H_2SO_4

$C_{inh.}$ (v/v %)	*IE*(%)									
	HCl					H_2SO_4				
	30°	40°	50°	60°	70°	30°	40°	50°	60°	70°
0.5	62.75	67.47	74.17	67.52	47.22	-16.49	-1.29	23.51	34.50	50.00
1.0	80.04	79.41	80.29	72.24	59.59	-6.91	21.15	36.64	38.29	63.96
2.0	83.91	82.08	83.16	81.28	69.13	19.14	30.07	43.24	53.39	74.09
5.0	87.62	88.51	90.44	86.35	85.95	25.75	38.34	52.57	64.54	79.14
10.0	90.60	88.89	91.25	91.21	92.27	53.21	62.44	72.64	73.64	88.33

Table 3 illustrates the variation of IE (%) with AEFL concentration at different temperatures in 2.0 M of HCl and H_2SO_4. The obtained data in Table 3 reveal that in both acids, the inhibition efficiency increased with an increase in the inhibitor concentration. This suggests that the inhibitor species are adsorbed on the mild steel/solution interface where the adsorbed species mechanically screen the coated part of the metal surface from the action of the corrosive medium.

As observed from Table 3, the effect of temperature on the inhibition efficiency of the studied inhibitor at all concentrations and temperatures shows two behavioral aspects depending on the type of the studied acid solution as follows:

1) In 2.0 M HCl solutions, an increase or decrease in the inhibitor efficiency depending on its concentration was detected with increasing temperature indicating that adsorption of inhibitor species on mild steel surface at these conditions is not merely physical or chemical adsorption but obeying a comprehensive adsorption (physical and chemical adsorption) [16].
2) In 2.0 M H_2SO_4 solutions, remarkable increase in the inhibitor efficiency was observed with increasing temperature up to 70° C. This increasing efficiency with increase in temperature is suggestive chemical adsorption mechanism which effectively enhanced with rising temperature [17].

The effect of temperature on the inhibited acid-metal reaction is highly complex, because many change occur on the metal surface such as rapid etching and desorption of inhibitor and the inhibitor itself may undergo decomposition and/or rearrangement. However, it was found that few inhibitors with acid-metal systems have specific reactions which are effective at high temperature as (or more) they are at low temperature [17-20].

In general, the data in Table 3 revealed that AEFL behaves in 2.0 M HCl better than in 2.0 M H_2SO_4. Several observations of such enhanced efficiency demonstrated by organic inhibitors of mild steel corrosion in HCl solutions as compared in H_2SO_4 solutions have been reported [11, 21-24] and may be attributed to the fact that chloride ions being less hydrated than sulphate ions are strongly adsorbed on the metal surface by creating an excess negative charge towards the solution phase, which favors synergistic adsorption on the metal surface.

3.3. Adsorption isotherms

The primary step in action of inhibitors in acid solutions is generally agreed to be adsorption on to the metal surface, which is usually oxide free in acid solutions. The adsorption of an inhibitor species, *Inh.*, on the metal surface in aqueous solutions should be considered a place exchanger reaction:

$$Inh._{aq.} + xH_2O_{ads.} \Leftrightarrow Inh._{ads.} + xH_2O_{aq.} \quad (4)$$

where x, the size ratio, is the number of water molecules displaced by one molecule of organic inhibitor. When the equilibrium of the process described in equation (4) is reached, it is possible to

obtain different expressions of the adsorption isotherm plots, and thus the degree of surface coverage ($\Theta = \frac{IE\ (\%)}{100}$) can be plotted as a function of the concentration of the inhibitor under test. It is worthwhile that at all studied temperatures the degree of surface coverage varies with the AEFL concentration following the Langmiur [25] adsorption isotherm in 2.0 M HCl (see Fig. 2) and Temkin [26] adsorption isotherm in 2.0 M H_2SO_4 (see Fig. 3). Langmuir and Temkin mathematical expressions are given as follows, respectively:

$$\frac{C_{inh.}}{\Theta} = \frac{1}{K_{e.c.a.}} + C_{inh.} \tag{5}$$

$$\Theta = \frac{1}{f}\ln K_{e.c.a.} + \frac{1}{f}\ln C_{inh.} \tag{6}$$

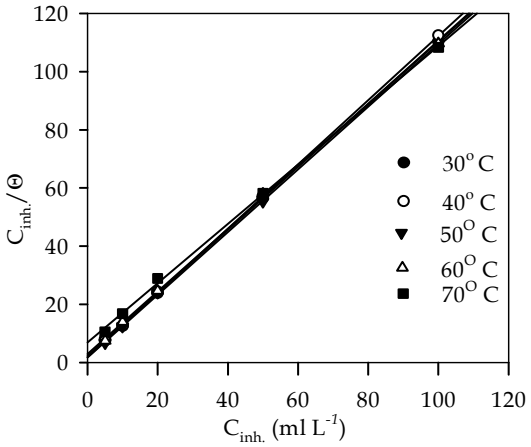

Figure 2. Langmuir adsorption isotherm of AEFL on mild steel surface in 2.0 M HCl.

where $C_{inh.}$ is the inhibitor bulk concentration in ml L^{-1}, $K_{e.c.a.}$ (ml^{-1} L) is the equilibrium constant of adsorption and f is the Temkin heterogeneity factor which is related to Frumkin lateral interaction factor a ($f = -2a$). The factor a describing the molecular interactions in the adsorbed layer. It can have both positive and negative values. The positive values of a indicates attraction forces between the adsorbed molecules while the negative values indicates repulsive forces between the adsorbed molecules. The adsorption parameters from both Langmuir and Temkin adsorption isotherms are estimated and listed in Tables 3 and 4, respectively. The obtained data in Tables 3 and 4 can be given as follows:

- The experimental data give good curves fitting for the applied adsorption isotherms as the correlation coefficients (r^2) were in the range $0.999 \geq r^2 \geq o.946$.
- As the adsorption isotherm in 2.0 M HCl is of Langmuir-type with slope of almost unity, monolayer of the inhibitor species must have been attached to mild steel surface without lateral interaction between the adsorbed species.

- As the adsorption isotherm in 2.0 M H_2SO_4 is of Temkin-type with negative values of factor a, repulsive forces between the adsorbed species on mild steel surface are expected.
- $K_{e.c.a.}$ value increases with temperature in both acids except in the case of HCl where it tends to decrease with the increase of temperature from 50° to 70° C.

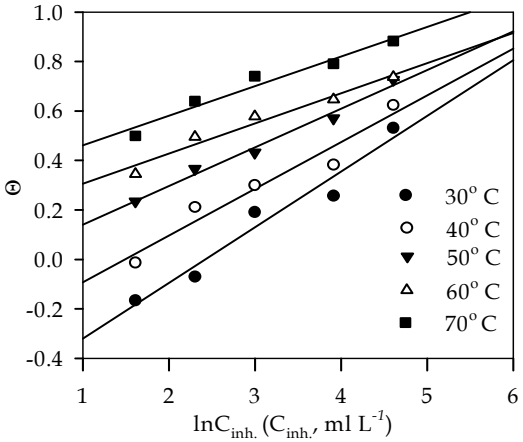

Figure 3. Temkin adsorption isotherm of AEFL on mild steel surface in 2.0 M H_2SO_4.

Table 4. Adsorption parameters for AEFL in 2.0 M HCl obtained from Langmuir adsorption isotherm at different temperatures.

Temperature	Adsorption parameters		
(°C)	slope	$K_{e.c.a.}$ (ml^{-1} L)	r^2
30°	1.1	0.445	0.999
40°	1.1	0.562	0.999
50°	1.1	0.578	0.999
60°	1.1	0.336	0.999
70°	1.0	0.146	0.999

Table 5. Adsorption parameters for AEFL in 2.0 M H_2SO_4 obtained from Temkin adsorption isotherm at different temperatures.

Temperature	Adsorption parameters			
(°C)	1/f	a	$K_{e.c.a.}$ (ml^{-1} L)	r^2
30°	0.225	-2.22	0.089	0.955
40°	0.189	-2.65	0.226	0.946
50°	0.156	-3.21	0.907	0.986
60°	0.122	-4.10	4.519	0.963
70°	0.120	-4.17	17.288	0.957

3.4. Thermodynamic adsorption parameters

The well known thermodynamic adsorption parameters are the free energy of adsorption ($\Delta G_{ads.}$), the heat of adsorption ($\Delta H_{ads.}$) and the entropy of adsorption ($\Delta S_{ads.}$). These quantities can be calculated by various mathematical methods depending on the estimated values of $K_{e.c.a.}$ from adsorption isotherms, at different temperatures as follows:

3.4.1. Method (I)

The $\Delta G_{ads.}$ values at all studied temperatures can be calculated from the following equation [27]:

$$K_{e.c.a.} = \frac{1}{C_{H_2O}} \exp(-\frac{\Delta G_{ads.}}{RT}) \quad (7)$$

where C_{H_2O} is the concentration of water molecules (in ml L^{-1}) at metal/solution interface. Then, the obtained $\Delta G_{ads.}$ values are plotted *versus* T (Fig. 4) in accordance with the basic equation [28]:

$$\Delta G_{ads.} = \Delta H_{ads.} - T\Delta S_{ads.} \quad (8)$$

A straight lines of intercept represents the $\Delta H_{ads.}$ values. By introducing the obtained $\Delta H_{ads.}$ values in Equation 8, $\Delta S_{ads.}$ values are calculate at all studied temperatures. As observed from Fig. 4, a segmented straight line of tow opposite slopes was obtained in 2.0 M HCl indicating the existence of tow sets of adsorption sites with different energetic heat of adsorption leading to the occurrence of comprehensive adsorption. All estimated thermodynamic adsorption parameters for AEFL on mild steel from 2.0 M of HCl and H_2SO_4 solutions were listed in Table 6.

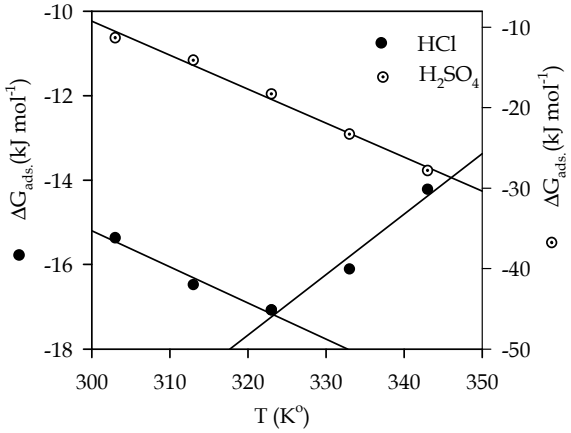

Figure 4. the variation of $\Delta G_{ads.}$ with T.

Table 6. Thermodynamic parameters for the adsorption of AEFL on mild steel in 2.0 M of both HCl and M H_2SO_4 at different temperatures.

Temperature	Thermodynamic adsorption parameters					
	HCl			H_2SO_4		
(°C)	ΔG_{ads} kJ mol^{-1}	ΔH_{ads} kJ mol^{-1}	ΔS_{ads} kJ $mol^{-1}K^{-1}$	ΔG_{ads} kJ mol^{-1}	ΔH_{ads} kJ mol^{-1}	ΔS_{ads} kJ $mol^{-1}K^{-1}$
Method (I)						
30°	-15.37	10.45	0.085	-11.31	116.59	0.422
40°	-16.48	10.45	0.086	-14.11	116.59	0.418
50°	-17.08	10.45, -63.42	0.085, -0.143	-18.29	116.59	0.418
60°	-16.11	-63.42	-0.142	-23.31	116.59	0.420
70°	-14.22	-63.42	-0.143	-27.83	116.59	0.421
Method (II)						
30°	-15.37	10.62	0.086	-11.31	116.59	0.422
40°	-16.48	10.62	0.087	-14.11	116.59	0.418
50°	-17.08	10.62, -63.12	0.086, -0.143	-18.29	116.59	0.418
60°	-16.11	-63.12	-0.141	-23.31	116.59	0.420
70°	-14.22	-63.12	-0.143	-27.83	116.59	0.421
Method (III)						
30°	1.93	10.72	0.029	6.02	116.61	0.365
40°	1.64	10.72	0.029	3.93	116.61	0.360
50°	1.35, 1.37	10.72, -63.23	0.029, -0.200	0.33	116.61	0.360
60°	3.37	-63.23	-0.200	-4.27	116.61	0.363
70°	5.37	-63.23	-0.200	-8.24	116.61	0.364
Method (IV)						
30°	-15.34	10.72	0.086	-11.26	116.61	0.422
40°	-16.51	10.72	0.087	-14.22	116.61	0.418
50°	-17.06, -17.36	10.72, -63.23	0.086, -0.142	-18.40	116.61	0.418
60°	-15.94	-63.23	-0.142	-23.25	116.61	0.420
70°	-14.18	-63.23	-0.143	-27.79	116.61	0.421
Method (V)						
30°	-15.37	10.72	0.086	-11.31	116.61	0.422
40°	-16.48	10.72	0.087	-14.11	116.61	0.418
50°	-17.08	10.72, -63.23	0.087, -0.143	-18.29	116.61	0.418
60°	-16.11	-63.23	-0.142	-23.31	116.61	0.420
70°	-14.22	-63.23	-0.143	-27.83	116.61	0.421

3.4.2. Method (II)

Gibbs-Helmholtz equation is [29]:

$$\left(\frac{\partial(\Delta G_{ads.}/T)}{\partial T}\right)_P = -\frac{\Delta H_{ads.}}{T^2} \tag{9}$$

The following equation can be derived from Eq. (9)

$$\int \frac{\partial(\Delta G_{ads.})}{T} = -\int \frac{\Delta H_{ads.}}{T^2} dT \tag{10}$$

It can be written the following equation from Eq. (10):

$$\frac{\Delta G_{ads.}}{T} = \frac{\Delta H_{ads.}}{T} + cons\tan t \tag{11}$$

By plotting $\frac{\Delta G_{ads.}}{T}$ *versus* $\frac{1}{T}$ (see Fig. 5), straight lines with slope represents the value of $\Delta H_{ads.}$. In 2.0 M HCl, a segmented straight line is also obtained. It must be pointed out that the values of $\Delta G_{ads.}$ were calculated as in **method (I)** from Eq. (7). By applying Eq. (8), $\Delta S_{ads.}$ values were calculated for all studied systems. All estimated thermodynamic adsorption parameters for AEFL on mild steel from 2.0 M of HCl and H_2SO_4 solutions were listed in Table 6.

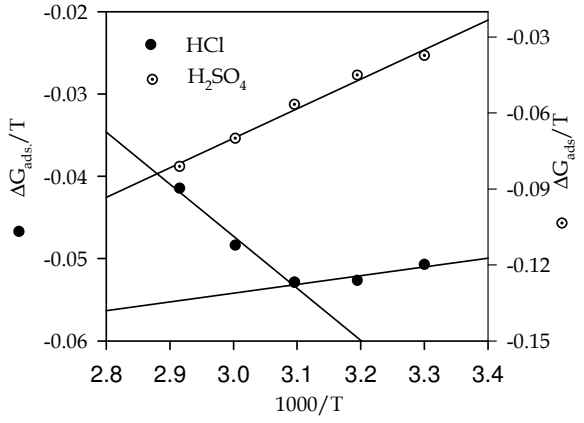

Figure 5. The variation of $\frac{\Delta G_{ads.}}{T}$ with $\frac{1}{T}$.

3.4.3. Method (III)

The dependence of the $K_{e.c.a.}$ values on the temperature can be given by the equation [30]:

$$K_{e.c.a.} = \exp(\frac{\Delta S_{ads.}}{R}) \exp(-\frac{\Delta H_{ads.}}{RT}) \tag{12}$$

which can be written in the form:

$$\log K_{e.c.a.} = \frac{\Delta S_{ads.}}{2.303R} - \frac{\Delta H_{ads.}}{2.303RT} \tag{13}$$

By plotting $\log K_{e.c.a.}$ *versus* $\frac{1}{T}$ (see Fig. 6), a straight lines of slope $-\frac{\Delta H_{ads.}}{2.303R}$ are obtained. In 2.0 M HCl, a segmented straight line is also obtained. The estimated $\Delta H_{ads.}$ values were introduced in Eq. (13) in order to calculate the corresponding $\Delta S_{ads.}$ at all studied temperatures. Then the obtained $\Delta H_{ads.}$ and $\Delta S_{ads.}$ were used to calculate $\Delta G_{ads.}$ with the help of Eq. (8). All estimated thermodynamic adsorption parameters for the studied inhibitor on mild steel from 2.0 M of HCl and H_2SO_4 solutions were listed in Table 6.

3.4.4. Method (IV)

By substituted the term $\Delta G_{ads.}$ in Eq. (7) with the equal terms in Eq. (8) the following equation can be obtained:

$$K_{e.c.a.} = \frac{1}{C_{H_2O}} \exp\left(\frac{\Delta S_{ads.}}{R} - \frac{\Delta H_{ads.}}{RT}\right) \tag{14}$$

which can be written as follows:

$$\log K_{e.c.a.} = \left(-\log C_{H_2O} + \frac{\Delta S_{ads.}}{2.303R}\right) - \frac{\Delta H_{ads.}}{2.303RT} \tag{15}$$

Equation (15) is similar to Eq. (13) except the intercept, where a new term was introduced in the intercept of Equation (15), this is $-\log C_{H_2O}$. Figure 6 represents also the relation in Eq. (15) in both acids. The $\Delta H_{ads.}$, $\Delta S_{ads.}$ and $\Delta G_{ads.}$ values for the inhibitor adsorption on mild steel in 2.0 M of HCl and H_2SO_4 were calculated as in **Method (III)** and the resultant data were listed in Table 6.

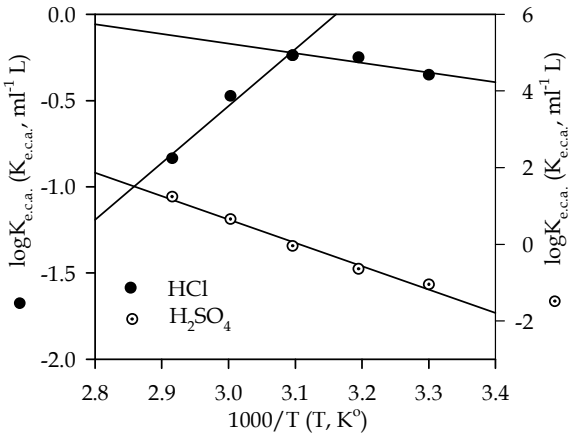

Figure 6. The variation of $\log K_{e.c.a.}$ with $\frac{1}{T}$.

3.4.5. Method (V)

The heat of adsorption ($\Delta H_{ads.}$) could be calculated according to the Van't Hoff equation [31]:

$$\log K_{e.c.a.} = -\frac{\Delta H_{ads.}}{2.303 \times RT} + cons\tan t \quad (16)$$

Figure 6 also represents the above relation where the slope of the resultant straight lines gives the value of $\Delta H_{ads.}$ in both acids. The $\Delta G_{ads.}$ and $\Delta S_{ads.}$ values in both acids were estimated from Eqs. (7 and 8), respectively. All the obtained values of $\Delta H_{ads.}$, $\Delta S_{ads.}$ and $\Delta G_{ads.}$ for the inhibitor adsorption on mild steel in both acids were listed in Table 6.

Inspection of the data recorded in Table 6, it was found that the thermodynamic parameters estimated by various methods are almost the same with the exception of $\Delta G_{ads.}$ and $\Delta S_{ads.}$ values calculated from **Method (III)** as their values deviated considerably from those obtained from the other methods. This result indicates that **method (III)** is not advisable for $\Delta G_{ads.}$ and $\Delta S_{ads.}$ calculations. **Method (III)** can be used only for $\Delta H_{ads.}$ calculations, while $\Delta S^{o}_{ads.}$ and $\Delta G_{ads.}$ can be estimated in accordance with Eqs. (7 and 8). So, it must be noted that $\Delta G_{ads.}$ and $\Delta S_{ads.}$ values calculated from **Method (III)** and recorded in Table 6 are not involved in the following discussions.

In general, the negative values of $\Delta G_{ads.}$ reflect that the adsorption of the AEFL species on mild steel surface from both acids is spontaneous process [32-34]. The dependence of $\Delta G_{ads.}$ on experimental temperature can be summarized in tow cases as follows:

a) $\Delta G_{ads.}$ may increase (becomes less negative) with increasing temperature indicating the occurrence of exothermic process at which adsorption was unfavorable with increasing reaction temperature as the result of the inhibitor desorption from the steel surface [34].
b) $\Delta G_{ads.}$ may decrease (becomes more negative) with increasing temperature indicating the occurrence of endothermic process at which increasing temperature facilitates inhibitor adsorption.

Both the two above cases (a and b) are observed for the adsorption of the studied inhibitor species on mild steel surface from HCl solution depending on the applied temperature range (see Table 6), indicating the occurrence of both endothermic and exothermic adsorption processes. While in H_2SO_4 solution, case (b) is only observed, indicating that the adsorption of inhibitor species is mainly occurred by endothermic process.

Moreover, the value of adsorption heat ($\Delta H_{ads.}$) gives valuable information about the mechanism of inhibitor adsorption. According to the recorded values of $\Delta H_{ads.}$ in Table (6) the following results can be obtained:

- In 2.0 M HCl solutions, both endothermic ($\Delta H_{ads.} = 10.72$ kJ mol^{-1}) and exothermic ($\Delta H_{ads.} = -63.23$ kJ mol^{-1}) adsorption behaviour were detected depending on the exact range of

applied temperatures. The average value of $\Delta H_{ads.}$ is about -26.26 kJ mol^{-1} which is larger than the common physical adsorption heat, but smaller than the common chemical adsorption heat [35], probably meaning that both physical and chemical adsorption take place (i.e. comprehensive adsorption). That is to say, since the adsorption heat approached the general chemical reaction heat, the chemical adsorption might occur accompanied by physical adsorption (electrostatic interaction).

- In 2.0M H_2SO_4 solutions, a large, positive value of $\Delta H_{ads.}$ (116.59 kJ mol^{-1}) was observed in the studied range of temperatures showing that the corrosion inhibition of mild steel in such solutions proceeds by chemical adsorption for the studied inhibitor species on the metal surface. This observation is in good agreement with those of Barrow [36] and Talati and Modi [37]. These reports state that the heat of chemical adsorption should be greater than 80 kJ mol^{-1}.

More interesting behaviour was observed in Table (6) that positive $\Delta S_{ads.}$ values is accompanied with endothermic adsorption process while negative $\Delta S_{ads.}$ values is accompanied with exothermic adsorption process. This is agrees with what expected, when the adsorption is an exothermic process, it must be accompanied by a decrease in the entropy energy change and vies versa [38].

3.5. Kinetic-thermodynamic corrosion parameters

As noticed previously, the adsorption process was well elucidate by using a thermodynamic model, in addition a kinetic-thermodynamic model was another tool to explain the mechanism of corrosion inhibition for an inhibitor.

Table 7. Kinetic-thermodynamic corrosion parameters for mild steel corrosion in absence and presence of various concentrations of AEFL.

$C_{inh.}$ (v/v %)	Kinetic corrosion parameters			
	A (g.cm^{-2}.min^{-1})	$E^*_{app.}$ (kJ mol^{-1})	ΔH^* (kJ mol^{-1})	ΔS^* (kJ mol^{-1}K^{-1})
HCl				
0.0	1.047×10^{8}	74.33	71.67	-0.100
0.5	2.951×10^{8}	79.89	77.22	-0.091
1.0	57.544×10^{8}	88.83	86.15	-0.067
2.0	14.454×10^{8}	85.73	83.05	-0.079
5.0	0.468×10^{8}	77.80	75.14	-0.107
10.0	0.013×10^{8}	69.01	66.35	-0.137
H_2SO_4				
0.0	1.585×10^{8}	76.76	74.08	-0.097
0.5	2.691×10^{4}	54.27	51.58	-0.169
1.0	2.138×10^{4}	54.15	51.49	-0.171
2.0	1.122×10^{4}	52.94	50.26	-0.176
5.0	0.339×10^{4}	50.19	47.58	-0.186
10.0	0.195×10^{4}	49.96	47.28	-0.191

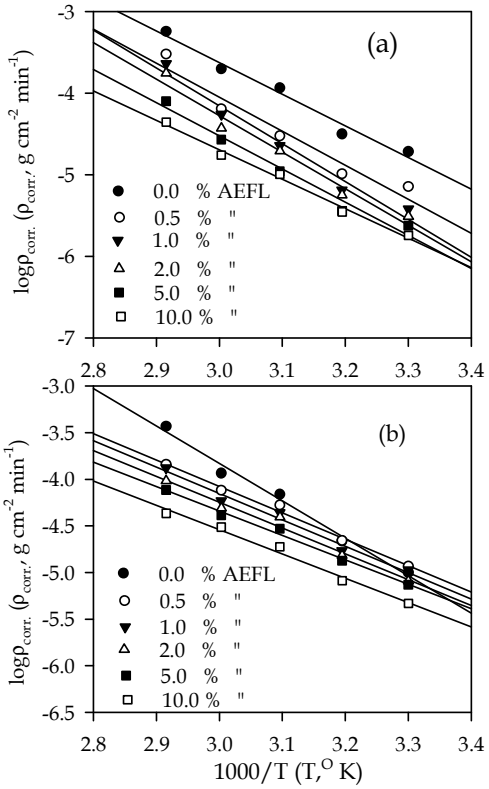

Figure 7. Arrhenius plots for mild steel corrosion rates ($\rho_{corr.}$) in (a) 2.0 M HCl and (b) H_2SO_4 in absence and presence of various concentrations of AEFL.

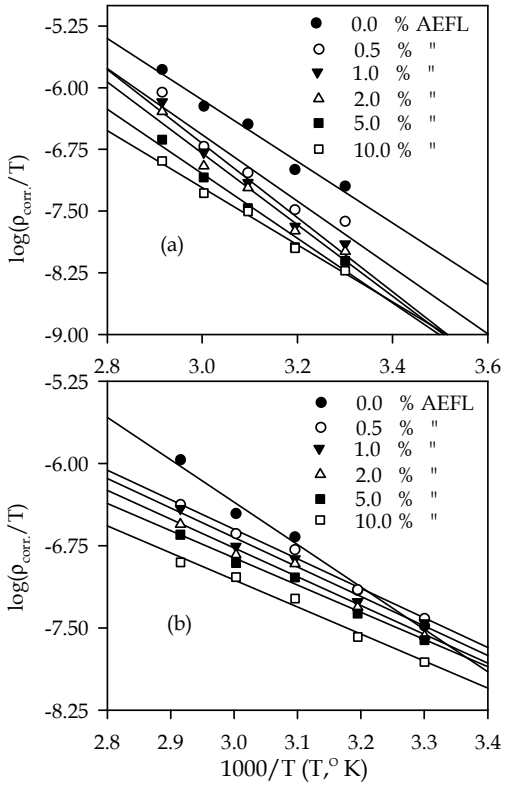

Figure 8. Transition-state plots for mild steel corrosion rates ($\rho_{corr.}$) in (a) 2.0 M HCl and (b) H_2SO_4 in absence and presence of various concentrations of AEFL.

The apparent effective activation energies ($E^*_{app.}$) for the corrosion reaction of mild steel in both acids in the absence and presence of different concentrations of AEFL were calculated from Arrhenius-type equation [39]:

$$\log \rho_{corr.} = \log A - \frac{E^*_{app.}}{2.303RT} \tag{17}$$

where A is the Arrhenius pre-exponential factor. A plot of $\log \rho_{corr.}$ *versus* $\frac{1}{T}$ gave straight lines as shown in Fig. 7. The enthalpy of activation (ΔH^*) and the entropy of activation (ΔS^*) for the intermediate complex in the transition state for the corrosion of mild steel in both acids in the absence and presence of different concentrations of AEFL were obtained by applying the transition-state equation [39]:

$$\log(\frac{\rho_{corr.}}{T}) = [(\log(\frac{R}{hN})) + (\frac{\Delta S^*}{2.303R})] - \frac{\Delta H^*}{2.303RT} \tag{18}$$

where h is the Plank's constant and N is the Avogadro's number. A plot of $\log(\frac{\rho_{corr.}}{T})$ *versus* $\frac{1}{T}$ should give a straight lines (see Fig. 8) with a slope of $(-\frac{\Delta H^*}{2.303R})$ and an intercept of $[(\log(\frac{R}{hN})) + (\frac{\Delta S^*}{2.303R})]$ from which the values of ΔH^* and ΔS^* were calculated, respectively. All estimated kinetic-thermodynamic parameters were tabulated in Table 7. The obtained data in Table 7 can be interpreted as follows:

- In 2.0 M HCl solutions, the addition of AEFL led to an increase in the apparent activation energy to values greater than that of the uninhibited solution (except that at 10.0 v/v%), suggesting that higher energy barrier for the corrosion process in the inhibited solutions associated with physical adsorption or weak chemical boding between the inhibitor species and the steel surface [7, 31]. Figure 9 illustrates the dependence of the apparent activation energy on the inhibitor concentration. The value of $E^*_{app.}$ increases with the increase in inhibitor concentration until reaches maximum value (88.83 kJ mol^{-1}) at concentration of 1.0 v/v% after which a decrease in the $E^*_{app.}$ value was observed with inhibitor concentration, but it was still higher than that of the uninhibited solution except for the higher level of inhibition (10 v/v%) as the detected $E^*_{app.}$ value was somewhat lower than that of the uninhibited solutions. The decrease in the $E^*_{app.}$ value at higher level of inhibitor efficiency was reported in the literature [31,33, 34]. Earlier explanation for this behaviour reported by Riggs and Hurd [40] was that at higher levels of inhibition the net corrosion reaction shifts from that on the uncovered part of the metal surface to the covered one. While unchanged or lowered $E^*_{app.}$ in inhibited solutions compared to the uninhibited one has been reported [39, 41, 42] to be indicative of chemical adsorption mechanism, as a result of which a surface film is formed and the surface area of the

metal covered by inhibitor species increases as temperature rises. These observations further support the occurrence of both physical and chemical adsorption for AEFL species on mild steel surface from HCl solutions.

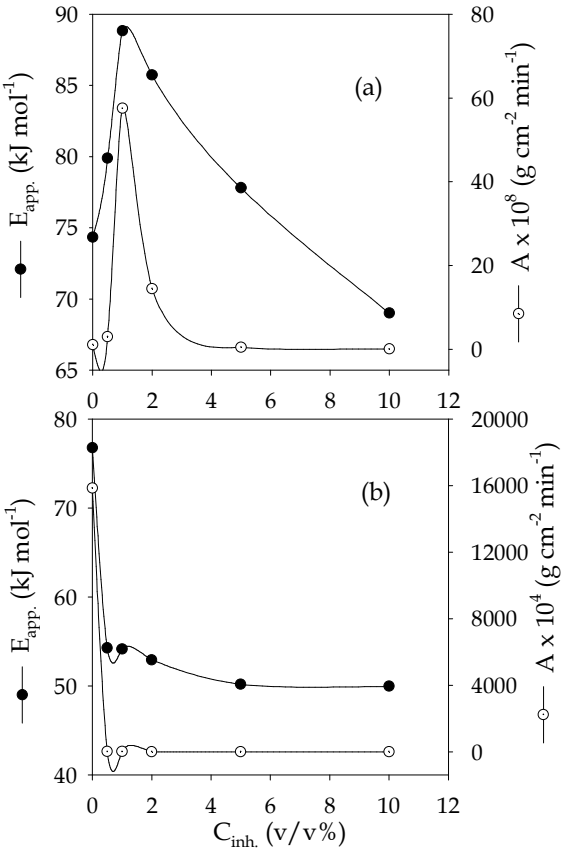

Figure 9. The relation of $E^*_{app.}$ and A with the concentration of AEFL in (a) 2.0 M HCl and (b) H_2SO_4.

- In 2.0 M H_2SO_4 solutions, the addition of AEFL led to abrupt decrease in the apparent activation energy to a value lower than that of the uninhibited solution and followed by monotonous decrease with the increase of inhibitor concentration (see Fig. 9), indicating that the inhibitory action of AEFL for mild steel corrosion in 2.0 M H_2SO_4 solutions occurs via chemical adsorption.
- In both acids, the tendency of variation in pre-exponential factor (A) was found to be similar to that in apparent activation energy (see Fig. 9). Similar results had been observed by some researchers [31, 34, 43]. In fact, the increase in the pre-exponential factor leads to an increase in corrosion rate. In the present study, it was found that the higher pre-exponential factors are associated with higher apparent activation energies, while the lower pre-exponential factors are associated with lower activation energies. Accordingly, good inhibitive properties for the studied inhibitor were observed even at conditions of lowest corrosion activation energies.
- In both acids, all values of $E^*_{app.}$ are larger than the analogous values of ΔH^* indicating that the corrosion process must involved a gaseous reaction, simply the hydrogen evolution reaction,

associated with a decrease in the total reaction volume. Moreover, for all systems, the average value of the difference $E_a - \Delta H^*$ is about 2.67 kJ mol^{-1} which approximately around the average value of RT (2.69 kJ mol^{-1}); where T are in the range of the experimental temperatures, indicating that the corrosion process is a unimolecular reaction as it is characterized by the following equation [44]:

$$E_a - \Delta H^* = RT \tag{19}$$

- The entropy of activation (ΔS^*) in the absence and presence of inhibitor has negative values. This indicates that the activated complex in the rate determining step represents an association rather than dissociation, meaning that, a decrease in disordering takes place on going from reactants to the activated complex [32, 45]. It is obviously that the ΔS^* shifts to more negative values (more ordered behaviour) with increasing inhibition efficiency and this was more pronounced in the case of H_2SO_4 inhibited solutions. This can be explained that the inhibitor species may involved in the activated complex of the corrosion reaction leading to more ordered systems.

3.6. Inhibitor constituents and inhibition mechanism

Fenugreek plant is native to the area from the eastern Mediterranean to Central Asia and Ethiopia, and much cultivated in Pakistan, India and China [46]. Fenugreek is also employed as a herbal medicine in many part of the world. However, numerous animal studies and preliminary trials in humans have found that fenugreek seeds and leaves can lower blood glucose and cholesterol levels and also have an anti-diabetic effect [47-49]. So, as commonly eaten food, fenugreek is generally regarded as safe [50]. Fenugreek leaves are rich with the following organic substances [51]:

- ascorbic acid ($C_6H_8O_6$),
- beta-carotene ($C_{40}H_{56}$),
- xanthophylls ($C_{40}H_{54}(OH)_2$),
- choline ($\overset{+}{N}(CH)_3C_2H_4OH$) and
- methionine ($HOOCCHNH_2CH_2CH_2SCH_3$).

As noticed, these substances are O-, N- and/or S-containing organic compounds. Ascorbic acid and beta-carotene will be excluded from this discussion as an investigation [52] revealed that the concentration of these compounds were remarkably reduced by storage and cooking (i.e. boiling). Sulphur-containing compounds are only of minor importance as inhibitor additives in HCl but they are frequently used in H_2SO_4 [1]. As a rule of thumb it holds that S-containing inhibitors are primarily useful in H_2SO_4, whilst N-containing inhibitors exert their best efficiencies in HCl. Some investigations reported that some N-containing compounds such as quaternary ammonium salts [53],

amino acids [54], and aliphatic amines [55] are relatively ineffective in prevention corrosion of iron and steel in H_2SO_4 solutions unless certain anions, especially halide (except fluoride) and pseudo-halide ions, are present. This long known synergistic effect [56] is widely used in inhibitor formulation. Trabanelli *et al.* [53] pointed out that N-decyl-pyridinium derivatives are good inhibitors in H_2SO_4 only when the inhibitor concentration is considerably larger than that used in HCl. Abdel Rahim *et al* [54] observed that even at higher level of methionine concentration (1.0×10^{-3} mol L^{-1}), it inhibits the corrosion of mild steel in H_2SO_4 by 55.3 % at 30^o C while with increasing temperature some increase in the inhibition efficiency was observed. According to these observations one can suggest that both choline and methionine compounds in Fenugreek leaves may play an important role in the corrosion inhibition of mild steel in HCl and H_2SO_4.

In acid inhibited solutions by AEFL, The choline compound is already in the cationic form and can be designed by (A^+) while the methionine compound may exist in tow forms:

- the neutral form which can be designed by (B) and
- the protonated form which can be designed by (HB^+).

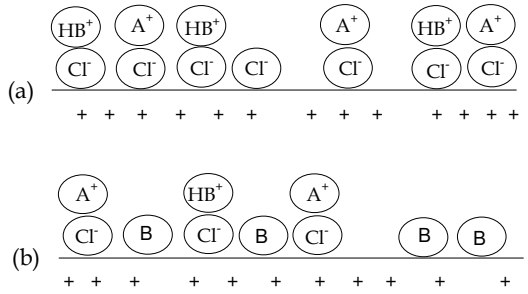

Figure 10. Schematic diagram of (a) cooperative and (b) competitave adsorption of Inhibitor species and Cl^-.

Many mechanisms have been proposed for the adsorption of organic inhibitors on a metal surface. The process of adsorption of inhibitors are influenced by the nature of the metal surface, the chemical structure of the organic inhibitor, the type of the aggressive electrolyte and the interaction between organic molecules and the metallic surface [57, 58]. The possibility of cation adsorption by means of electrostatic forces is determined by the electric charge of the metal surface with respect to the solution. Since steel surface contained positive charges acid media [10], the good inhibitive properties of the AEFL in HCl could be explained by the occurrence of joint adsorption between the cationic species and Cl^- ions . It has been suggested that two types of joint adsorption take place [59]:

1) **Cooperative adsorption**: at which A^+ and HB^+ cations are adsorbed on the sites where the Cl^- is already adsorbed on the negatively charged metal surface (see Fig. 10a). This represents physical adsorption for the onium ions on the Cl^- bridge formed on mild steel surface. This

mechanism may occur obviously at lower inhibitor concentrations at which desorption for the inhibitor species was facilitated with increasing temperature

2) **Competitive adsorption**: at higher level of inhibitor concentration (10 v/v%), inhibitor species of type HB^+ may be compete with the Cl^- to adsorbed on different sites of steel surface at which they neutralized and adsorbed through coordinate bond by partial transference of electrons from the polar atom (N and/or S) to the metal surface (see Fig. 10b). Here, the chemical adsorption is occurred. But still the inhibitor species originally of cation type (A^+) and some of the protonated type (HB^+) were adsorbed physically on the Cl^- bridge formed on mild steel surface. Accordingly comprehensive adsorption is clear cut.

On the other hand, the situation in H_2SO_4 inhibited solutions is different as the heavily, large hydrated ions of sulphate are weakly adsorbed on the negatively charged steel surface. So, under low concentrations of AEFL, joint adsorption of cationic species with SO_4^{2-} was not sufficient to protect the metal surface from the attack of the aggressive solution and the cation HB^+ may do ***free delivery service*** to transport the H^+ from the bulk solution to the metal surface at which the following reaction may occur:

$$HB^+ + e^- \Rightarrow B + 1/2H_2 \tag{20}$$

Hence an acceleration behaviour is observed in 2.0M H_2SO_4 solutions containing lower inhibitor concentration. This behaviour disappeared with increasing both inhibitor concentration and temperature. Increasing inhibitor concentration led to a competitive adsorption between inhibitor species (A^+ and HB^+) and the SO_4^{2-} ions. As HB^+ species reach the metal/solution interface, they subsequently neutralized with the formation of molecules, with consequence chemical adsorption through a lone pair of the hetero atom (i.e. N and./or S). The role of the inhibitor cation of type A^+ was assumed to be negligible under this conditions. With increasing solution temperature, inhibitor species move rabidly and receive the interface more quickly and hence chemical adsorption of B species occurs successfully which is enhanced by raising temperature.

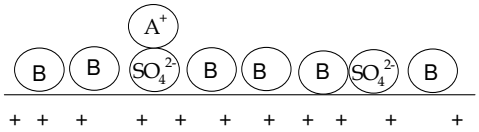

Figure 11. Schematic diagram of adsorption of Inhibitor species and SO_4^{2-} on mild steel surface.

4. CONCLUSIONS

1) In 2.0M HCl, the inhibition efficiency of AEFL increases with increasing concentration, while an increase or decrease in the inhibitor efficiency is detected with increasing temperature depending on AEFL concentration.

2) In 2.0M H_2SO_4, the inhibition efficiency of AEFL increases with increasing AEFL concentration and solution temperature.
3) The AEFL inhibits mild steel corrosion in HCl more than in H_2SO_4 at all inhibitor concentrations and solution temperatures.
4) The inhibition action of AEFL is performed via adsorption of the extract species on mild steel surface. The adsorption is spontaneous and follows Langmuir adsorption isotherm in HCl, while follows Temkin adsorption isotherm in in H_2SO_4 at all studied temperatures.
5) Thermodynamic data for both inhibitor adsorption and mild steel corrosion led to suggest the occurrence of (i) comprehensive adsorption (physical and chemical adsorption) for the inhibitor species on mild steel from HCl solution and (ii) chemical adsorption for the inhibitor species on mild steel from H_2SO_4 solution.
6) The inhibition mechanism for the adsorption of AEFL species on mild steel surface from both acids was discussed with the light of some AEFL constituents.

References

1. G. Schmitt, Br. *Corros. J.* 19 (1984) 165.
2. S. T. Arab and E. A. Noor, *Corrosion* (NACE) February (1993) 122.
3. Z. Jiang, J. Wang, Q. Hu and S. Huang, *Corros. Sci.* 37 (1995) 1245.
4. F. Bentiss, M. Traisnel, L. Gengembre and M. Lagrenee, *Appl. Surf. Sci.* 152 (1999) 237.
5. S. S. Abd El-Rehim. S. A. M. Refaey, F. Taha, M. B. Saleh and R. A. Ahmed, *J. Appl. Electrochem.* 31 (2001) 429.
6. S. T. Arab and A. M. Al-Turkustani, *Inter. J. Chem.* 12 (2002) 249.
7. A. Popova, E. Sokolova, S. Raicheva and M. Christov, *Corros, Sci*. 45 (2003) 33.
8. H.-L. Wang, H.-B. Fan and J.-S. Zheng, *Mater. Chem. Phys*. 77 (2003) 655.
9. M. Bouklah , N. Benchat , B. Hammouti , A. Aouniti , S. Kertit , *Mater. Letters* 60 (2006) 1901.
10. A. Popova, M. Christov and A. Vasilev, *Corros. Sci*. 49 (2007) 3290.
11. S. Muralidharan, M. A. Quraishi and. S. V. Iyer, *Burtugalia Chem. Acta* 11 (1993) 255.
12. S. Rengamani, S. Muralidharan, M. A. Kulandainathan and S. V. Iyer, *J. Appl. Electrochem*. 24 (1994) 355.
13. S. Muralidharan, M. A. Quraishi and. S. V. Iyer, *Corros. Sci*. 37 (1995) 1739.
14. E. Khamis, M. A. Ameer, N. M. Al-Andis and G. Al-Senani, *Corrosion* (NACE) 56 (2000) 127.
15. E. A. Noor, *Corros. Sci*. 47 (2005) 33.
16. B. A. Abd-El-Nabey, E. Khamis, M. Sh. Ramadan and A. El-Gindy, *Corrosion* (NACE) 52 (1996) 671.
17. B. I. Ita and O. E. Offiong, *Mater. Chem. Phys*. 70 (2001) 330.
18. S.N. Raicheva, E. Sokolova and A. E. Stoyanova, *Bulgarian Chem. Commun*. 27 (1994) 363.
19. M. M. Singh and A. Gupta, *Bull. Electrochem*. 12 (1996) 511.
20. M. H. Wahdan, A. A. Hermas and M. S. Morad, *Mater. Chem. Phys*. 76 (2002) 111.
21. T. Vasudevan, S. Muralidharan, S. Alwarappan and S. V. Iyer, *Corros. Sci*. 37 (1995) 1235.
22. L. Elkadi, B. Mernari, M. Traisnel, F. Bentiss and M. Lagrenee, *Corros. Sci*. 42 (2000) 703.
23. T. Y. Soror and M. A. El-Ziady, *Mater. Chem. Phys*. 77 (2002) 697.
24. M. A. Quraishi and D. Jamal, *Mater. Chem. Phys*. 78 (2003) 608.
25. I. Langmuir, J. Amer. *Chem. Soc*. 39 (1947) 1848.
26. M. I. Temkin, *Zh. Fiz. Khim* 15 (1941) 296.
27. E. Khamis, *Corrosion* (NACE) 46 (1990) 476.

28. A. A. El-Awady, B. Abd El-Nabey and S. G. Aziz, *Electrochem. Soc*. 139 (1992) 2149.
29. S. Bilgic, *Mater. Chem. Phys*. 76 (2002) 52.
30. S. S. Abd El-Rehim, H. H. Hassan and M. A. Amin, *Corros. Sci*. 46 (2004)5.
31. X. Li and G. Mu, *Appl. Surf. Sci.* 252 (2005) 1254.
32. S. S. Abd El-Rehim, H. H. Hassan and M. A. Amin, *Mater. Chem. Phys*. 70 (2001) 64.
33. L. Tang, X. Lie, Y. Si, G. Mu and G. Liu, Mater. *Chem. Phys*.95 (2006) 29.
34. L. Tang, G. Mu and G. Liu, *Corros. Sci*. 45 (2003) 2251.
35. G. Mu, X. Li and G. Liu, *Corros. Sci*. 47 (2005) 1932.
36. G. M. Barrow,Physical Chemistry, McGraw-Hill, New York, 4th Ed. (1983) 739.
37. J. D. Talati and R. M. Modi, *Trans. SAEST* 11 (1986) 295.
38. J. M. Thomas and W. J. Thomas, Introduction to the Principles of Heterogeneous Catalysis, 5th Ed, Academic Press, London (1981) 14.
39. I. N. Putilova, S. A. Balezin and V. P. Barannik, Metallic Corrosion Inhibitors, Pergamon Press, New York (1960) 31.
40. O.L. Riggs Jr. and R. M. Hurd, *Corrosion* 23 (1967) 252.
41. S. Martinez and I. Stern, *J. Appl Electrochem*. 31 (2001) 973.
42. S. S. Abd El-Rehim, M. A. M. Ibrahim and K. F. Khalid, *Mater. Chem. Phys*. 70 (2001) 268.
43. X. Li ans L. Tang, *Mater. Chem. Phys*. 90 (2005) 286.
44. K. J. Laidler, Reaction kinetics, Vol. 1, 1st Edn., Pergamon Press, New York (1963).
45. M. K. Gomma and M. H. Wahdan, *Mater. Chem. Phys*. 39 (1995) 209.
46. J. F. Morton, *J. Ethanopharm*. 29 (1990) 215.
47. A. Chevallier, The Encyclopedia of Medicinal Plants Dolrling Kindersley. London (1996) ISBN 9-780751-303148.
48. J. Raju, D. Gupta, A. R. Rao, P. K. Yadava and N. Z. Baquer, *Mol. Cell Biochem*. 224 (2001) 45.
49. B. Annide and P. Stanely Maizen Prince, *J. Med.Food* 7 (2004) 153.
50. R. D. Shama, A. Sarkar, D. K. Hazra, *et al Phytother. Res*. 10 (1996) 519.
51. www.swsbm.com/Constituents/constituentsQ-Z.html.
52. S. K. Yadav and S. Sehgal, *Plant Foods Hum. Nutr*. 50 (1997) 239.
53. G. Trabanelli, L. Meszaros, B. Lengyel, T. Garai and A. Frignani, Proceding of the 6th European Symposium on Corrosion Inhibitors (6SEIC) Ann. Univ. Ferrara, N. S., Sez. V (8) (1985) 473.
54. M. A. Abdel Rahim, H. B. Hassan and M. W. Khalil, Mat.-wiss., u. *Werkstofftech*. 28 (1997) 198.
55. A. S.Fouda, H. A. Mostafa, F. El-Taib and G. Y. Elewady, *Corros. Sci*. 47 (2005) 1988.
56. A. N. Frumkin, *Z. Elektrochem*. 59 (1955) 807.
57. S. Kertit, A. Elkhely, J. Aride, A. Srhiri, A. Brn-Bachir, M. Etman, *J. Appl. Electrocem*. 19 (1989) 83.
58. G. Banerjee, S. N. Malhatra, *Corrosion* 48 (1992) 10.
59. K. Aramaki, M. Hagiwara and H. Nishihara, *Corros. Sci*. 27 (1987) 487.